Dynamic characteristics of high-speed $In_{0.4}Ga_{0.6}As/GaAs$ self-organized quantum dot lasers at room temperature

S. Ghosh, S. Pradhan, and P. Bhattacharya[a]

Solid State Electronics Laboratory, Department of Electrical Engineering and Computer Science, University of Michigan, 1301 Beal Avenue, Ann Arbor, Michigan 48109-2122

(Received 19 July 2002; accepted 23 August 2002)

We have measured the room-temperature modulation characteristics of self-organized $In_{0.4}Ga_{0.6}As/GaAs$ quantum dot lasers in which electrons are injected into the dot lasing states by tunneling. A small-signal modulation bandwidth of $f_{-3\,dB}=22$ GHz is measured. Values of differential gain at 288 K of $dg/dn \cong 8.85\times10^{-14}$ cm^2 and gain compression factor $\varepsilon=7.2\times10^{-16}$ cm^3 are derived from the modulation data. Extremely low values of linewidth enhancement factor $\alpha\sim1$ and chirp <0.6 Å were also measured in the devices. [DOI: 10.1063/1.1514823]

Self-organized quantum dot (QD) lasers,[1] grown by molecular beam epitaxy (MBE) or metalorganic vapor phase epitaxy (MOVPE), have demonstrated attractive characteristics in recent years in terms of threshold current, wavelength tunability, and output power.[2–4] However, these devices have not helped researchers in the realization of a large modulation bandwidth at room temperature. Detailed two- and three-pulse pump–probe differential transmission spectroscopy measurements were made by us on QD laser heterostructures similar to separate confinement heterostructure (SCH) lasers.[5–8] These measurements were done both as a function of temperature (up to 300 K) and of injection carrier density. The results indicate that at high temperatures, a large number of injected electrons preferentially occupy the higher lying states of the dots and states in the adjoining barrier/wetting layer with higher density. The carrier relaxation times from the higher lying electronic states to the dot ground state levels, from which lasing is desired, are ~50–100 ps at room temperature.[7,8] It is therefore apparent that there may be a significant ''hot carrier'' problem that leads to gain compression and other related deleterious effects in QD lasers at room temperature. As the temperature is lowered, the hot carrier distribution is minimized and carriers relax from the higher lying states by efficient electron-hole scattering.[9] In fact, we have recorded small-signal modulation bandwidths of ~30 GHz in QD SCH lasers at 80 K,[10] while in the same devices, the highest measured $f_{-3\,dB}\cong7.5$ GHz at 300 K.[9]

In a conventional SCH device, while injected carriers lose energy and fill the lasing states, carrier heating simultaneously forces them out towards higher energies and causes leakage to adjoining layers. In QD lasers, these problems can become worse due to the effects discussed above. On the other hand, if electrons are introduced directly into the lasing states by tunneling and the tunneling rate is comparable to the stimulated emission rate, the carrier distribution in the active region will remain ''cold'' and hot carrier effects are minimized. It is important to note that the hole relaxation rates in QDs and in other quantum confined structures are very large due to the multiplicity of the levels, band mixing, and efficient hole–phonon coupling. Enhanced performance in tunneling injection quantum well lasers has been reported in the past,[11,12] and more recently, improvements in tunnel injection QD laser characteristics and temperature dependence of the threshold current have been experimentally demonstrated and theoretically predicted.[13–15] In this letter, we report the measured high-speed characteristics of high-performance tunnel injection $In_{0.4}Ga_{0.6}As/GaAs$ self-organized QD lasers. We demonstrate small-signal modulation bandwidths larger than 20 GHz at room temperature in these devices, together with ultralow chirp and the linewidth enhancement factor.

The QD laser heterostructure was grown by MBE and the conduction band profile is illustrated in Fig. 1(a). The 95 Å $In_{0.25}Ga_{0.75}As$ injector well is grown at 490 °C, the three coupled QD layers are grown at 525 °C, and the rest of the structure is grown at 620 °C. The samples exhibit luminescence peaks at 1.26 and 1.3 eV from the QDs and from the $In_{0.25}Ga_{0.75}As$ quantum well injector, respectively. The wavelength of the dot luminescence peak is controlled by adjusting the InGaAs dot charge during epitaxy. The energy separation in the conduction band between the injector well states and the QD ground states is ~36 meV at room temperature. This energy separation ensures longitudinal optical (LO) phonon-assisted tunneling from the injector well to the dot ground states through the 20 Å $Al_{0.55}Ga_{0.45}As$ barrier layer. An interesting observation was made in that the photoluminescence linewidth for the ground state quantum dot transition in the tunneling injection structures was always quite small. The linewidth (23 meV at 20 K) is almost a factor of 2–3 lower than that measured in conventional coupled quantum dot heterostructures. We believe that the tunneling process helps to *select* the dots that contribute to the lasing process and this filtering adds to the homogeneity of the dot size.

Ridge waveguide lasers 3 μm$\times$400 μm long were fabricated by standard lithography, wet and dry etching, and metallization techniques. The cleaved facets were left uncoated. The threshold current of the device with continuous-wave (cw) biasing is 12 mA at room temperature. The measured light–current characteristics under pulsed biasing condition (1 μs with 1% duty cycle) are shown in Fig. 1(b).

[a]Electronic mail: pkb@eecs.umich.edu

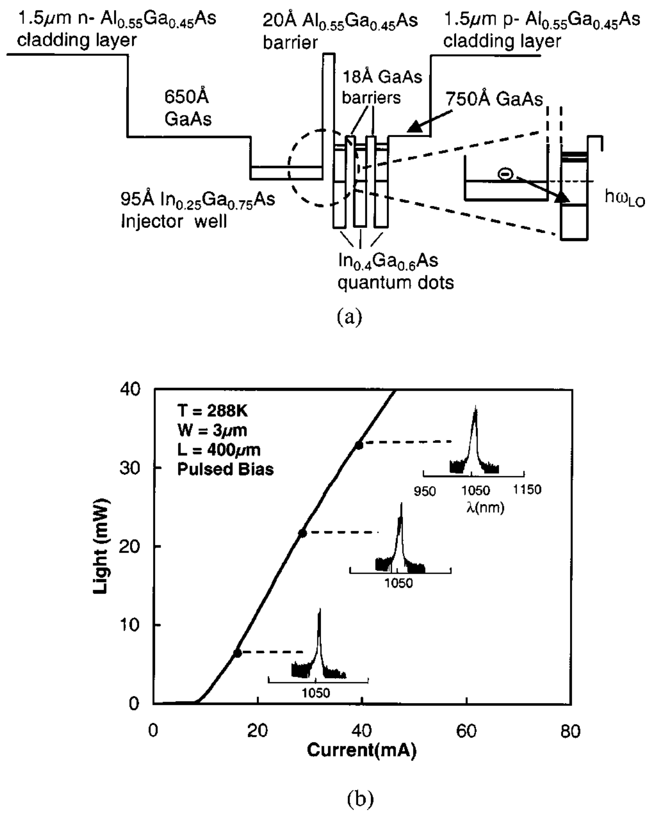

FIG. 1. (a) Conduction band profile of the tunnel injection quantum dot laser heterostructure under flat-band conditions; (b) measured light–current characteristics of a single-mode tunnel injection quantum dot laser. The insets depict the spectral outputs at various currents.

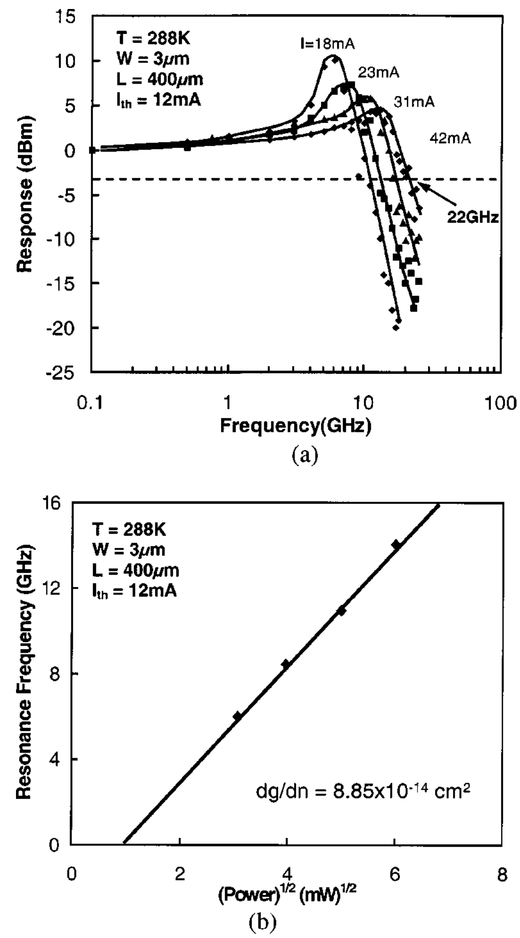

FIG. 2. (a) Small-signal modulation response with varying injection currents at 288 K; (b) plot of resonance frequency f_r of the modulation response vs the square root of the output power.

High values of slope efficiency (0.86 W/A) and differential quantum efficiency ($\eta_d = 0.73$) are measured in these devices. From measurements on lasers with varying cavity lengths, an internal quantum efficiency of $\eta_i = 0.85$ and cavity loss coefficient of $\gamma = 8.2\ \mathrm{cm}^{-1}$ are derived. The lasing peak wavelength under threshold conditions is recorded at 1.069 μm (1.16 eV).

The small-signal modulation response of the devices was measured at room temperature under cw biasing conditions with a HP 8562A electrical spectrum analyzer, a HP 8350B sweep oscillator, a low noise amplifier, and a New Focus high-speed detector. The frequency response for varying injection currents is shown in Fig. 2(a). The continuous lines are guides for the eye. Shown as insets in Fig. 1(b) are the spectral outputs at these injection currents, which confirm that lasing from the ground state is maintained. A bandwidth of $f_{-3\,\mathrm{dB}} = 22$ GHz is measured for $I \sim 42$ mA and this is the highest bandwidth measured in any QD laser at room temperature. The modulation response shows gain compression limited behavior and analysis of the modulation data gives us a gain compression factor of $\epsilon = 7 \times 10^{-16}\ \mathrm{cm}^3$. This value is a factor of 10 larger than those measured in the best quantum well lasers.[11,16] Figure 2(b) shows the plot of the resonance frequency f_r of the modulation response as a function of the square root of the output power. The modulation efficiency, which is the slope of this plot, is $\sim$2.7 GHz/mW$^{1/2}$. From this value of modulation efficiency and using a dot fill factor of $\sim$28% and a confinement factor $\Gamma \sim 2.5 \times 10^{-3}$, we derive the value of differential gain, $dg/dn = 8.85 \times 10^{-14}\ \mathrm{cm}^2$, at room temperature. This value of differential gain is higher than those measured in separate confinement heterostructure QD lasers grown under identical conditions.[10]

The linewidth enhancement factor, α, is expressed as

$$\alpha = -\frac{4\pi}{\lambda}\frac{dn/dN}{dg/dN}, \tag{1}$$

where N is the carrier density, n is the refractive index, and g is the gain. The linewidth enhancement factors as a function of frequency were obtained by measuring the subthreshold emission spectra of the single-mode tunnel injection ridge waveguide lasers and by calculating the Fabry-Pérot mode peak-to-valley ratios and shifts between two differential bias currents. The Fabry-Pérot mode shifting due to heating was minimized by using a pulsed bias (1 μs pulse width and 10 kHz repetition rate). Shown in Fig. 3(a) is the wavelength (frequency) dependence of the linewidth enhancement factor. We measure a maximum value of $\alpha \cong 1.2$ at the lasing wavelength. These values of α, which agree with those reported by Newell *et al.*[17] for SCH-QD lasers, suggest that the emission linewidth of these quantum dot lasers approaches the Schawlow–Townes limit. The trend observed in the data as a function of wavelength is explained by the fact that, in the tunnel injection laser, most of the carriers are injected into the lasing state and the carrier distribution remains quasi-Fermi. Therefore, the carrier-induced change in refractive index is expected to be maximum at or near the lasing wavelength. The values of α are a factor of 2–5 lower than those

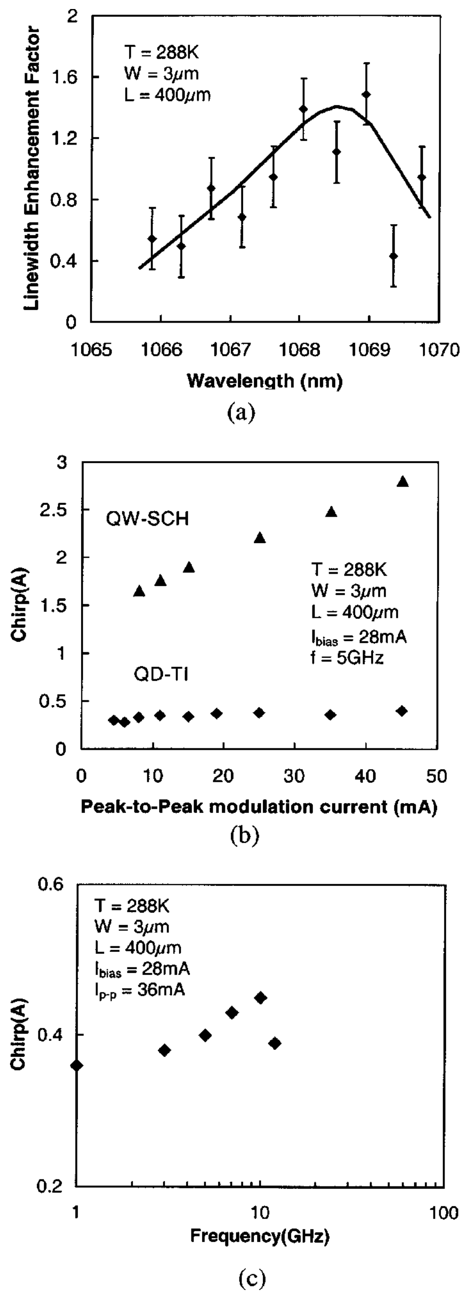

FIG. 3. (a) Measured linewidth enhancement factor vs wavelength; (b) plots of chirp measured in the tunnel injection quantum dot laser and a SCH quantum well laser as a function of the modulation current; (c) chirp measured as a function of the modulation frequency in a tunnel injection quantum dot laser.

measured in SCH quantum well lasers[18] and this is largely attributed to the higher differential gain and a smaller carrier-induced modulation of the refractive index in the active volume.

The chirp in a semiconductor laser is directly proportional to the linewidth enhancement factor α. We have measured the chirp in the tunnel injection QD lasers during direct small-signal modulation at room temperature by measuring the broadening of a single longitudinal mode using an optical spectrum analyzer. Lasing was confirmed to be at the ground state wavelength. The sinusoidal modulation current was superimposed on a pulsed dc bias current. The envelope of the dynamic shift in the wavelength was recorded and the difference between the half width of the observed envelope with and without modulation was used to evaluate the chirp. The resolution of the optical spectrum analyzer was 0.08 nm. The measurements were first done at a frequency of 5 GHz with a pulsed dc bias of 28 mA and the peak-to-peak modulation current (I_{p-p}) was varied from 4.2 to 42 mA. The data are shown in Fig. 3(b). Chirp in an $In_{0.25}Ga_{0.75}As$ SCH quantum well laser of identical cavity dimensions and similar threshold current was also measured under identical conditions and the data are also displayed in Fig. 3(b). The values of chirp in the quantum well laser are comparable to those reported earlier.[19] In Fig. 3(c) we show the chirp measured in the quantum dot devices as a function of modulation frequency. It is evident from the data of Figs. 3(b) and 3(c) that chirp in the tunnel injection QD lasers is almost nonexistent and at the noise level of the measurements, even at high modulation frequencies. This behavior also confirms the reduction in hot carrier density in the active volume of the lasers. The low chirp also follows from the small linewidth enhancement factor in these devices.

The authors acknowledge useful discussions with Professor D. Bimberg. The work was supported by the Army Research Office under Grant No. DAAD019-01-1-0331.

[1] D. Bimberg, M. Grundmann, and N. N. Ledenstov, *Quantum Dot Heterostructures* (Wiley, Chichester, UK, 1998).
[2] G. T. Liu, A. Stintz, H. Li, K. J. Malloy, and L. F. Lester, Electron. Lett. **35**, 1163 (1999).
[3] P. M. Varangis, H. Li, G. T. Liu, T. C. Newell, A. Stintz, B. Fuchs, K. J. Malloy, and L. F. Lester, Electron. Lett. **36**, 1544 (2000).
[4] D. Bimberg, M. Grundmann, F. Heinrichsdorff, N. N. Ledentsov, V. M. Ustinov, A. E. Zhukov, A. R. Kovsh, M. V. Maximov, Y. M. Shernyakov, B. V. Volovik, A. F. Tasul'nikov, P. S. Kop'ev, and Zh. I. Alferov, Thin Solid Films **367**, 235 (2000).
[5] T. Sosnowski, T. Norris, H. Jiang, J. Singh, K. Kamath, and P. Bhattacharya, Phys. Rev. B **57**, R9423 (1998).
[6] J. Urayama, T. Norris, J. Singh, and P. Bhattacharya, Phys. Rev. Lett. **86**, 4930 (2001).
[7] K. Kim, T. Norris, and P. Bhattacharya, 14th Annual Meeting of the Lasers and Electro-Optics Society (LEOS), San Diego, 2001.
[8] J. Urayama, T. Norris, H. Jiang, J. Singh, and P. Bhattacharya, Appl. Phys. Lett. **80**, 2162 (2002).
[9] P. Bhattacharya, K. Kamath, J. Singh, D. Klotzkin, J. Phillips, H.-T. Jiang, N. Chervela, T. Norris, T. Sosnowski, J. Laskar, and M. Ramana Murty, IEEE Trans. Electron Devices **46**, 871 (1999).
[10] D. Klotzkin, K. Kamath, K. Vineberg, P. Bhattacharya, R. Murty, and J. Laskar, IEEE Photonics Technol. Lett. **10**, 932 (1998).
[11] H. Yoon, H. C. Sun, and P. Bhattacharya, Electron. Lett. **30**, 1675 (1994).
[12] P. Bhattacharya, J. Singh, H. Yoon, X. Zhang, A. Gutierrez-Aitken, and Y. Lam, IEEE J. Quantum Electron. **32**, 1620 (1996).
[13] L. Asryan and S. Luryi, IEEE J. Quantum Electron. **37**, 905 (2001).
[14] G. Walter, N. Holonyak, Jr., J. H. Ryou, and R. D. Dupuis, Appl. Phys. Lett. **79**, 3215 (2001).
[15] P. Bhattacharya and S. Ghosh, Appl. Phys. Lett. **80**, 3482 (2002).
[16] D. Klotzkin and P. Bhattacharya, IEEE J. Lightwave Technol. **17**, 1634 (1999).
[17] T. C. Newell, D. J. Bossert, A. Stintz, B. Fuchs, K. J. Malloy, and L. F. Lester, IEEE Photonics Technol. Lett. **11**, 1527 (1999).
[18] J. Stohs, D. Bossert, D. Gallant, and S. Brueck, IEEE J. Quantum Electron. **37**, 1449 (2001).
[19] H. Saito, K. Nishi, and S. Sugou, Electron. Lett. **37**, 1293 (2001).